DOI: 10.1002/chem.200700583

Self-Assembled Single-Walled Carbon Nanotube:Zinc–Porphyrin Hybrids through Ammonium Ion–Crown Ether Interaction: Construction and Electron Transfer

Francis D'Souza,*[a] Raghu Chitta,[a] Atula S. D. Sandanayaka,[b] Navaneetha K. Subbaiyan,[a] Lawrence D'Souza,[c] Yasuyuki Araki,[b] and Osamu Ito*[b]

Abstract: An ammonium ion–crown ether interaction has been successfully used to construct porphyrin–single-walled carbon nanotube (SWNT) donor–acceptor hybrids. The [18]crown-6 to alkyl ammonium ion binding strategy resulted in porphyrin–SWNT nanohybrids that are stable and soluble in DMF. The porphyrin–SWNT hybrids were characterized by spectroscopic, TEM, and electrochemical techniques. Both steady-state and time-resolved emission studies revealed efficient quenching of the singlet excited state of the porphyrins and free-energy calculations suggested that electron-transfer quenching occurred. Nanosecond transient absorption spectral results supported the charge-separation quenching process. Charge-stabilization was also observed for the nanohybrids in which the lifetime of the radical ion pairs was around 100 ns. The present nanohybrids were also used to reduce the hexyl viologen dication (HV^{2+}) and to oxidize 1-benzyl-1,4-dihydronicotinamide in solution in an electron-pooling experiment. Accumulation of the radical cation ($HV^{\bullet+}$) was observed in high yields, which provided additional proof for the occurrence of photoinduced charge separation. The present study demonstrates that a hydrogen-bonding motif is a successful self-assembly method to build SWNTs bearing donor–acceptor nanohybrids, which are useful for light-energy harvesting and photovoltaic applications.

Keywords: crown compounds · donor–acceptor systems · electron transfer · nanotubes · porphyrinoids

Introduction

Recently, major research efforts have been devoted to understand the physico-chemical properties of carbon nanotubes,[1] which are a new allotropic form of carbon, with the intention of developing nanometer-dimension materials and devices that could be used in future technologies.[2] In this context, single-walled carbon nanotubes (SWNTs) have emerged as attractive candidates because of their outstanding physical, chemical, and mechanical properties, together with their potential for practical applications. Additionally, SWNTs are better characterized and offer characteristic spectroscopic fingerprints compared with other forms of nanotubes.[1,2] SWNTs consist of graphitic layers wrapped seamlessly into cylinders that originate from defined sections of two-dimensional graphene sheets. The presence of these extended, delocalized π-electron systems makes SWNTs attractive candidates for developing efficient energy harvesting, photovoltaic, and hydrogen storage materials.[2,3] In this context, incorporating SWNTs into donor–acceptor ensembles for the study of light-induced electron transfer is

[a] Prof. F. D'Souza, R. Chitta, N. K. Subbaiyan
Department of Chemistry
Wichita State University
1845 Fairmount, Wichita
Kansas 67260-0051 (USA)
Fax: (+1) 316-978-3431
E-mail: Francis.DSouza@wichita.edu

[b] Dr. A. S. D. Sandanayaka, Dr. Y. Araki, Prof. O. Ito
Institute of Multidisciplinary Research for Advanced Materials
Tohoku University, Katahira
Aoba-ku, Sendai, 980-8577 (Japan)
Fax: (+81) 22-217-5610
E-mail: ito@tagen.tohoku.ac.jp

[c] Dr. L. D'Souza
Department of Chemical Engineering
University of Illinois at Chicago
810 S. Clinton, Chicago 60607 (USA)

Supporting information for this article is available on the WWW under http://www.chemeurj.org/ or from the author.

an active area of research.[3–5] A few elegant covalently linked[4] and noncovalently assembled[5] donor–acceptor hybrids that contain SWNTs have been developed. Among the covalent and noncovalent assembly methods, noncovalent methods are more appealing because these methods would not significantly perturb the electronic structure of the nanotubes. For this reason, noncovalent strategies are often adopted in the complex superstructures of biological systems. However, the use of well-defined self-assembly methods to develop SWNT-bearing donor–acceptor hybrids is still in its infancy. A few examples that involve π–π, van der Waals, electrostatic, and metal–ligand coordination interactions have recently been developed.[5]

Self-assembly by using an ammonium ion–crown ether interaction is a powerful method because it offers a high degree of directionality with binding energies of up to 100 kJ mol^{-1}.[6] However, to date, no ammonium ion–crown ether interactions have been used to assemble SWNTs bearing donor–acceptor hybrids, primarily owing to difficulties associated with the ammonium ion–crown ether self-assembly protocol. In the present study, the alkyl ammonium ion–crown ether binding interaction has been successfully used to self-assemble donor–acceptor hybrids. Our strategy, which involves the molecules shown in Scheme 1, includes the following steps:

1) For solubilization of SWNTs, we have adopted the well known SWNT–pyrene (Pyr) π-stacking method.[7] This method is especially suitable compared with chemical derivatization because it preserves the electronic structure of the SWNT.
2) To self-assemble donor entities, we functionalized the Pyr entity with an alkyl ammonium cation, **1**, and formed SWNT–**1** nanohybrids.
3) Next, alkyl ammonium cations were self-assembled by using an alkyl ammonium ion–crown ether binding interaction to porphyrins that contain one or four [18]crown-6 moieties. Porphyrins with a higher number of crown ether moieties are expected to result in more stable ensembles owing to the cooperative binding effect.

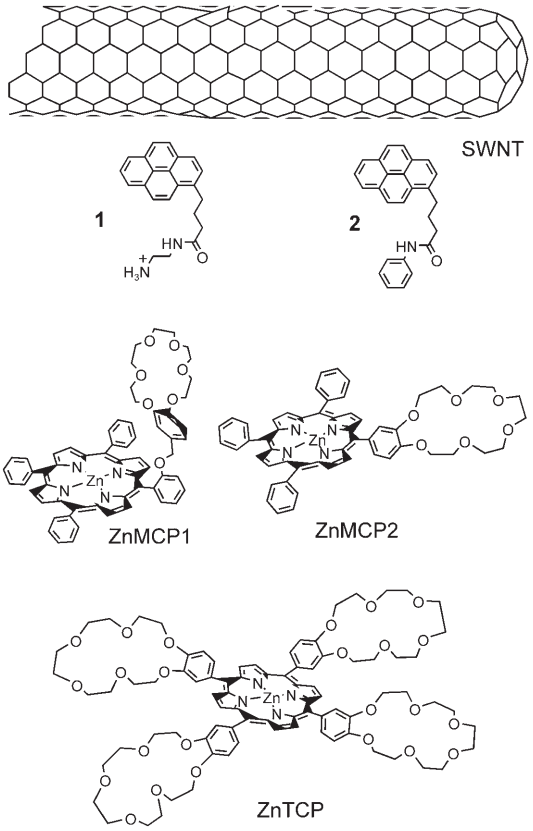

Scheme 1. Structures of the compounds investigated depicting the adopted self-assembly methodology.

Results and Discussion

Optical absorption and emission studies: The binding of **1** to a crown ether appended porphyrin (ZnCP) was investigated by using optical absorption methods in DMF. Addition of **1** to a solution of zinc–porphyrin that contained one crown ether moiety (ZnMCP1) (Scheme 1) resulted in a decrease in the Soret band intensity. The binding constant was evaluated by constructing a Benesi–Hildebrand plot[8] and was found to be $9.4\times10^{3}\,\text{M}^{-1}$, which suggests a moderate stability for the alkyl ammonium ion–crown ether assembled supramolecular complex (see Figure S1 in the Supporting Information for spectra and the plot).[9] As mentioned earlier, porphyrins that contain four crown ether moieties are expected to form much more stable supramolecular complexes (Figure 1) owing to the cooperative effect.

The absorption spectrum of the SWNT–**1** ensemble revealed bands that correspond to the nanotubes in the 400–600, 600–950, and 1100–1660 nm range, which indicates the presence of both metallic and semiconducting nanotubes in the sample[10] (see Figure S2 in the Supporting Information for the spectrum). The fine structures of the bands indicated

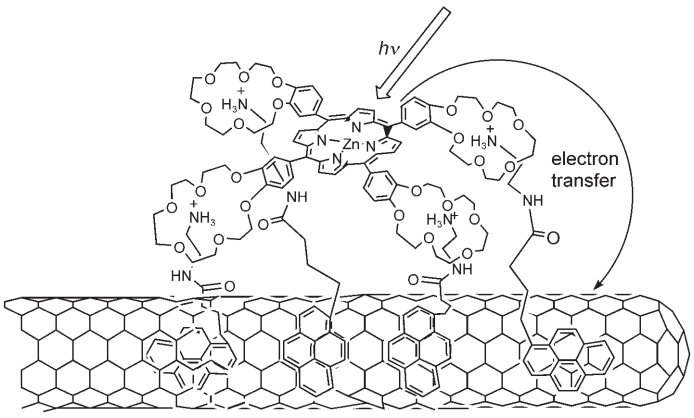

Figure 1. Strategy adopted for the construction of SWNT-**1**:ZnTCP hybrids in the present study and the photochemical events upon excitation of the porphyrin entity.

preservation of the electronic structure of the SWNT after immobilization with **1**. In the UV region, the samples also revealed peaks that correspond to the presence of pyrene entities. However, these bands were found to be broadened relative to pure **1**, perhaps as a result of π stacking with the SWNTs. The presence of the pyrene entity on the SWNT was also confirmed by recording the fluorescence spectrum of SWNT–**1** in DMF. When excited at 340 nm, which corresponds to one of the absorption peaks of pyrene, emission peaks that correspond to the pyrene entity were observed in the 375 to 430 nm range. However, the emission intensity was found to be quenched by more than 95% of the original intensity of **1** at the same pyrene concentration as a consequence of π–π stacking of pyrene on the nanotube (see Figure S3 in the Supporting Information for the spectra).

Figure 2 shows TEM images of SWNT–**1** in DMF. In agreement with literature results,[4,5] the SWNT bundles were found to be loosened after treatment with **1**, although some of them intertwine again during TEM sample preparation. This observation suggests an appreciable decrease in branches of several SWNTs stacked together compared with untreated, commercially available SWNTs of high purity. Additionally, most of the amorphous carbon and Fe nanoparticles present in the untreated SWNT were absent in solubilized SWNT–**1**. This result suggests that adsorbed **1** largely acts to separate the SWNTs and prevents them from stacking with each other.

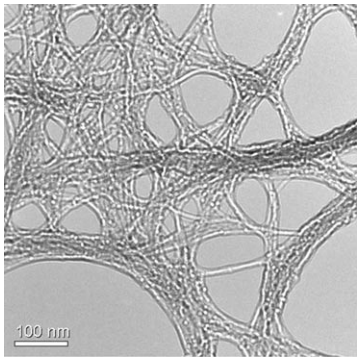

Figure 2. TEM image of SWNT–**1** dispersed in DMF.

The SWNT–**1**:ZnCP donor–acceptor hybrids were formed in solution by the addition of SWNT–**1** to either of the zinc–porphyrins that contained one crown ether moiety (ZnMCP1 or ZnMCP2). As shown in Figure 3a, addition of SWNT–**1** to a solution of a zinc–porphyrin that contains four crown ether moieties (ZnTCP, Scheme 1) in DMF revealed a diminished Soret band intensity at 430 nm accompanied by two isosbestic points at 423 and 438 nm, respectively. Similar spectral changes were observed when ZnMCP1 and ZnMCP2 were titrated with SWNT–**1** (See Figures S4a and S5a in the Supporting Information). Addition of SWNT–**1** was also found to efficiently quench the fluorescence of the ZnCPs. As shown in Figure 3b for ZnTCP, both emission bands of ZnP revealed quenching of more than 60% of their initial intensity. In a control experiment, SWNTs were also solubilized by using pyrene that contains a phenyl ring (**2** in Scheme 1) instead of the alkyl ammonium ion. When ZnCPs were titrated with SWNT–**2** no clear interaction was observed, that is, the decrease in the Soret intensity was minimal with no clear isosbestic points. Also, quenching of the ZnCP emission was less than 15%. These results clearly suggest the formation of a self-assembly through the alkyl ammonium ion–crown ether interaction, which is similar to that reported for the same series of ZnCPs interacting with alkyl ammonium cation-functionalized fullerenes.[9]

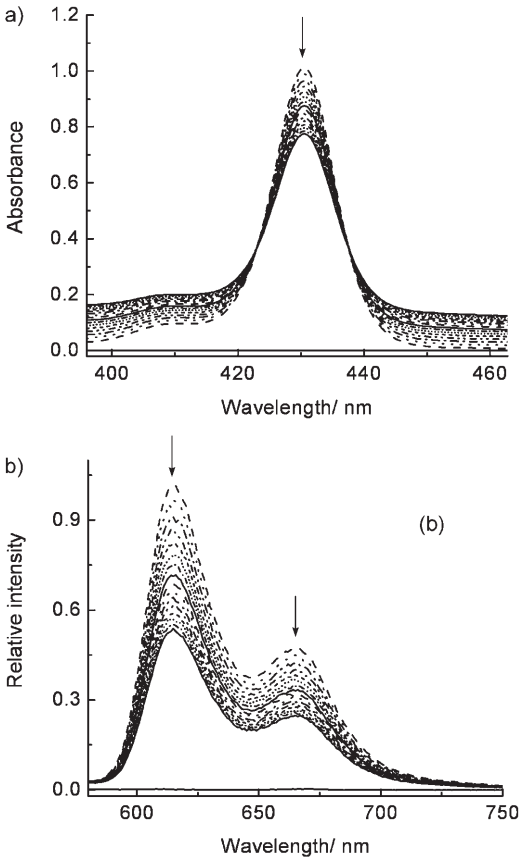

Figure 3. a) Absorption spectra in the Soret region and b) emission spectra of ZnTCP on adding increasing amounts of SWNT–**1** in DMF. λ_{ex} = 558 nm.

Electrochemical studies and electron-transfer driving force calculations: Electrochemical studies by using cyclic voltammetry were performed to understand the overall redox behavior of the SWNT–**1**:ZnCP nanohybrids and to evaluate the energetics of light-induced electron transfer. Figure 4 shows the cyclic voltammograms of ZnTCP with increasing amounts of SWNT–**1**. The first oxidation and first reduction of ZnTCP were located at $E_{1/2} = 0.76$ and -1.25 V versus Ag/AgCl, respectively. Addition of SWNT–**1** resulted in a small cathodic shift of the oxidation wave (≈ 30 mV) with increased peak-to-peak separation. The latter can be attributed to slow electron transfer in the SWNT–**1**:ZnCP nanohybrids as a result of limited access of the SWNT-

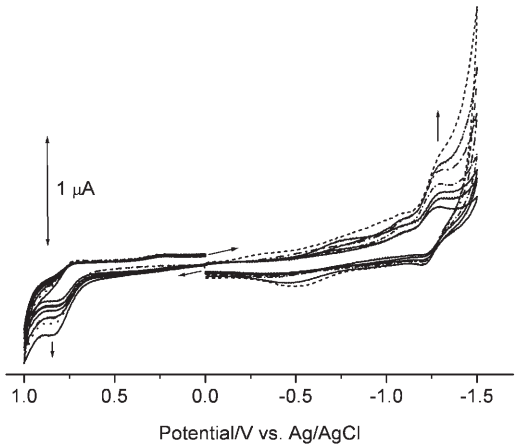

Figure 4. Cyclic voltammograms of ZnTCP (≈0.01 mM) upon adding increasing amounts of SWNT–**1** in DMF that contains 0.1 M $(n\text{Bu})_4\text{NClO}_4$. Scan rate = 100 mV s^{-1}.

bound redox probes to the electrode surface.[5g] The current that corresponds to SWNTs started emerging from around −0.3 V and increased as the applied negative potential increased.[11] It may be mentioned here that **1** did not exhibit any redox processes within the potential window of the solvent used. Similar electrochemical behavior was observed for nanohybrids constructed by using ZnMCP1 and ZnMCP2. The free-energy changes for charge separation, ΔG_{CS}, were calculated according to the Rehm–Weller method,[12] by employing the first oxidation potential of ZnCPs, the reduction potential of SWNTs (from the starting point potential of −0.3 V), the singlet excitation energy of ZnP (2.05 eV), and the estimated Coulomb energy. The ΔG_{CS} value for generating the radical ion pair $SWNT^{\bullet-}$–**1**:$ZnCP^{\bullet+}$ was found to be ≈−1.1 eV, which indicates the possibility of photoinduced charge separation in the nanohybrids.

Time-resolved emission and transient absorption studies: Further time-resolved emission and nanosecond transient absorption spectral studies were performed to understand the quenching process. The singlet excited state of the ZnCPs in DMF revealed a monoexponential decay with lifetimes of around 2 ns. These lifetimes were found to be efficiently decreased upon formation of the nanohybrids, as shown in Figure 5, for the representative SWNT–**1**:ZnTCP (see Figure S6 in the Supporting Information for other nanohybrids). The decay could be fitted satisfactorily to a biexponential decay curve for all of these nanohybrids, as determined from their χ^2 values. By assuming that the fast decaying components, which are in the 65 to 82% fractions, are a result of excited-state charge separation, the rate constants of charge separation (k_{CS}) were evaluated as given in Table 1. The magnitude of k_{CS} and the quantum yield (Φ_{CS}) suggests an efficient charge-separation process. On the other hand, the slower components in the 22 to 35% fraction were attributed to both the loosely bound ZnCP or unbound ZnCP entities in solution.

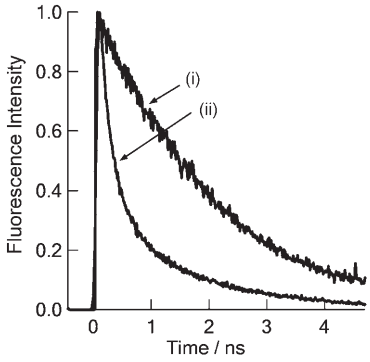

Figure 5. Fluorescence decays of ZnTCP (i) and SWNT–**1**:ZnTCP (ii) monitored at the 600–700 nm range. The porphyrin concentration was held at 0.01 mM (λ_{ex} = 400 nm).

Table 1. Fluorescence lifetimes, charge-separation rate constants (k_{CS}), and quantum yields (Φ_{CS}) for ^{1}ZnCP*, charge-recombination rate constants (k_{CR}), lifetimes of the radical ion pairs (τ_{RIP}) and percentage of maximal conversion of $HV^{+\bullet}$ from the added HV^{2+} for SWNT–**1**:ZnCP nanohybrids in DMF.

Donor[a]	τ_f [ps] (fraction [%])	k_{CS}[b] [s^{-1}]	Φ_{CS}[b]	k_{CR} [s^{-1}]	τ_{RIP} [ns]	Yield $HV^{\bullet+}$ [%]
ZnTCP	250 (78) 1500 (22)	3.5×10^9	0.87	5.1×10^6	190	92
ZnMCP1	230 (82) 1710 (28)	3.8×10^9	0.88	1.7×10^7	60	95
ZnMCP2	280 (65) 1570 (35)	3.1×10^9	0.86	1.1×10^7	90	94

[a] See Scheme 1 for structures. The lifetimes of reference ZnTCP, ZnMCP1 and ZnMCP2 were 1955, 1955, and 1975 ps, respectively, in DMF. [b] $k_{CS} = (1/\tau_f)_{sample} - (1/\tau_f)_{ref}$; $\Phi_{CS} = k_{CS}/(1/\tau_f)_{sample}$. $(\tau_f)_{sample}$ is the fast decay component and τ_{ref} is the lifetime of the respective ZnCP compound given in [a].

Further, nanosecond transient absorption spectral studies provided evidence for charge separation (Figure 6 and Figure S7 in the Supporting Information) and allowed us to estimate the charge recombination rates, k_{CR}. The transient spectra revealed peaks in the 460 nm range that are mainly a result of the triplet absorption of ZnCPs. The $ZnCP^{\bullet+}$, which was expected to appear in the 500 to 680 nm range, overlapped with the ZnCP triplet absorption bands.[4,5] There was also a broad peak at around 1400 nm that could be due to $SWNT^{\bullet-}$, although additional studies are warranted to confirm this assignment. It was possible to estimate the value of k_{CR} by monitoring the quick decay of $ZnCP^{\bullet+}$ at 660 nm because the slow decay part at 660 nm in Figure 6 (and the inset of Figure S7 in the Supporting Information) can be attributed to the tail of the overlapping ZnP triplets. The k_{CR} values evaluated are given in Table 1 along with the lifetimes of the radical ion pairs, τ_{RIP}, which were in the nanosecond range and suggest that there is charge stabilization in the SWNT–**1**:ZnCP nanohybrids reported herein.

Electron-pooling experiments: To authenticate the occurrence of photoinduced charge-separation in the donor–acceptor nanohybrids, electron-pooling experiments were conducted with the help of an electron mediator, hexyl viologen

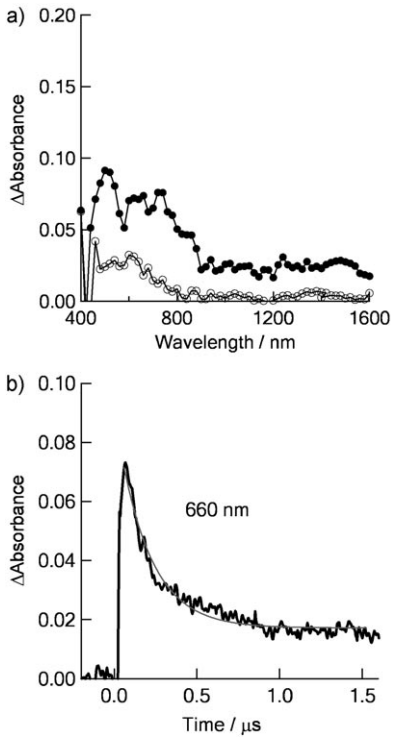

Figure 6. a) Nanosecond transient absorption spectra of SWNT–**1**:ZnTCP (0.01 mM) observed by laser irradiation at 532 nm (ca. 3 mJ per pulse) in DMF at 0.1 μs (●) and 1.0 μs (○) time intervals. b) Absorption–time profile monitored at 660 nm.

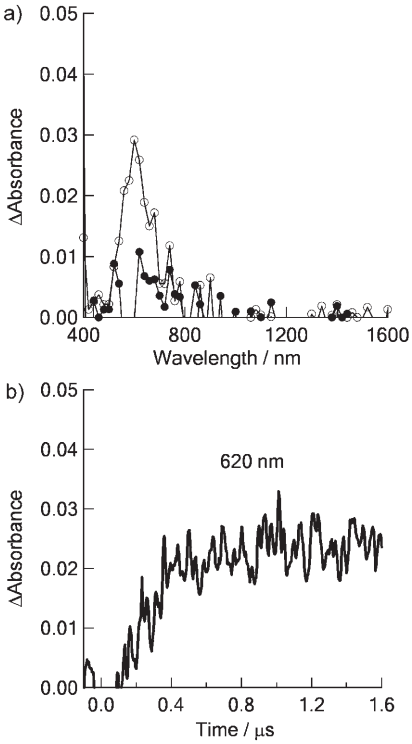

Figure 7. a) Nanosecond transient absorption spectra of SWNT–**1**:ZnMCP2 (0.01 mM) in the presence of HV^{2+} (0.5 mM) and BNAH (1.5 mM) observed by laser irradiation at 532 nm (ca. 3 mJ per pulse) in DMF at 0.1 μs (●) and 1.0 μs (○) time intervals. b) Absorption–time profile of the 620 nm peak.

dication (HV^{2+}), and an electron-hole shifter, 1-benzyl-1,4-dihydronicotinamide (BNAH).[13] As shown in Figure 7a (and Figure S8 in the Supporting Information), addition of HV^{2+} to a solution that contained SWNT–**1**:ZnCP nanohybrids revealed a transient absorption band at around 620 nm that corresponds to the reduced form of HV^{2+} ($HV^{\bullet+}$).[14] These results suggest that there is electron transfer from $SWNT^{\bullet-}$ to HV^{2+} and provide additional proof for the formation of one-electron reduced SWNTs. As expected, the time profile of the $HV^{\bullet+}$ band revealed rapid decay owing to charge-recombination with the hole on ZnCP (Figure 7b). Interestingly, addition of both HV^{2+} and BNAH to a solution that contained SWNT–**1**:ZnCP nanohybrids and exciting the sample by using 532 nm laser light, revealed the expected $HV^{\bullet+}$ radical band at 620 nm. The signal intensity of this radical peak did not decay appreciably over the microsecond timescale, which indicates that the hole from $ZnP^{\bullet+}$ shifts to BNAH to give the irreversible generation of 1-benzyl-1,4-nicotinamide (BNA^+) as the final product (Scheme 2).[5g,14]

To establish the occurrence of electron transfer leading to the persistent formation of the $HV^{\bullet+}$ radical, steady-state laser photolysis experiments were performed. Figure 8 (and Figure S9 in the Supporting Information) shows absorption spectral changes that illustrate the accumulation of $HV^{\bullet+}$ as a consequence of the photoinduced processes on addition of HV^{2+} and BNAH, as depicted in Scheme 2. For this reason, SWNT–**1**:ZnCP nanohybrids were repeatedly excited by

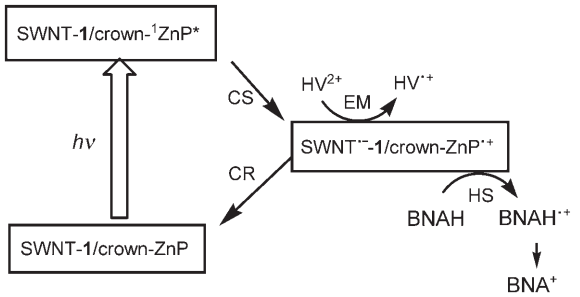

Scheme 2. Generation of $HV^{\bullet+}$, the radical cation and dehydrogenated forms of BNAH ($BNAH^{\bullet+}$ and BNA^+) from the photoexcited SWNT–**1**:ZnCP nanohybrids. Abbreviations: HV^{2+} and $HV^{\bullet+}$; hexyl viologen dication and its radical cation, CR; Charge recombination, EM; electron migration, and HS; hole shift.

using 532 nm laser light in the presence of HV^{2+} and BNAH. Accumulation of $HV^{\bullet+}$ was observed at around 620 nm, supporting the occurrence of the electron-mediating process. The $HV^{\bullet+}$ concentration increased with increasing the BNAH concentration as a result of the bimolecular nature of the hole-shift process. Also, an increase in HV^{2+} concentration increased the maximum $HV^{\bullet+}$ absorbance ($Abs(HV^{\bullet+})$). In a control experiment, upon irradiation of ZnCP in the absence of SWNT by using 532 nm laser light, the accumulation of $HV^{\bullet+}$ was negligible when similar concentrations of ZnCP, HV^{2+}, and BNAH were employed, thus supporting the importance of SWNTs as electron ac-

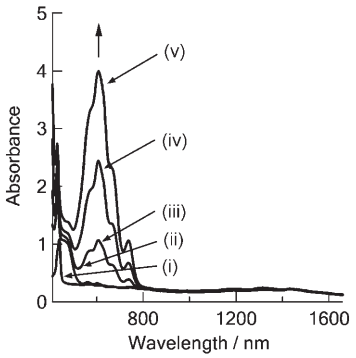

Figure 8. Steady-state absorption spectral changes of SWNT–**1**:ZnMCP1 (0.01 mM) in the presence of HV^{2+} (0.5 mM) and varying amounts of BNAH (in 0.05 cm cell length) before and after repeated 532 nm laser light irradiation (ca. 3 mJ per pulse). i) SWNT–**1**:ZnMCP1, ii) SWNT–**1**:ZnMCP1 and HV^{2+} (0.5 mM), iii) SWNT–**1**:ZnMCP1, HV^{2+} (0.5 mM) and BNAH (0.5 mM), iv) SWNT–**1**:ZnMCP1, HV^{2+} (0.5 mM) and BNAH (1.0 mM), and v) SWNT–**1**:ZnMCP1, HV^{2+} (0.5 mM) and BNAH (1.5 mM). All solutions are in deaerated DMF.

ceptors in the initial photoinduced charge-separation process. These results clearly demonstrate the occurrence of electron and hole mediation from the photogenerated $SWNT^{\bullet-}$–**1**:$ZnCP^{\bullet+}$ nanohybrid to HV^{2+} and BNAH, respectively. From the peak maxima of $HV^{\bullet+}$ obtained after repeated irradiation by using 532 nm laser light and by employing the reported molar extinction coefficient of the methyl viologen radical cation,[15] the conversion of HV^{2+} to $HV^{\bullet+}$ was evaluated to be 97 to 99% in DMF. These observations illustrate efficient photosensitized electron-transfer/electron-mediation processes of the donor–acceptor nanohybrids constructed by using the ammonium ion–crown ether self-assembly approach.

Conclusion

In conclusion, by utilizing the ammonium ion–crown ether binding motif, SWNT–ZnP donor–acceptor nanohybrids were constructed and characterized by spectroscopic, TEM, and electrochemical techniques. The [18]crown-6 to alkyl ammonium cation binding strategy adopted resulted in nanohybrids that are stable and soluble in DMF. Both steady-state and time-resolved emission studies revealed efficient quenching of the singlet excited state of the porphyrins and free-energy calculations suggested electron-transfer quenching. Nanosecond transient absorption spectral results were supportive of the charge-separation quenching process. Charge-stabilization was also observed for the nanohybrids in which the lifetime of the radical ion pairs was around 100 ns. The present nanohybrids were further utilized to reduce HV^{2+} and to oxidize BNAH in solution in an electron-pooling experiment. Accumulation of the radical cation $HV^{\bullet+}$ was observed in high yields, which offers additional proof for the occurrence of photoinduced charge separation. The present study demonstrates that the ammonium ion–crown ether binding motif is a successful self-assembly method to build SWNTs bearing donor–acceptor nanohybrids and are useful for light-energy conversion and photovoltaic applications.

Experimental Section

Chemicals: SWNTs (HiPco) were obtained from Carbon Nanotech (Houston, TX). All of the reagents were from Aldrich Chemicals (Milwaukee, WI), whereas the bulk solvents used in the syntheses were from Fischer Chemicals. Tetrabutylammonium perchloride, nBu$_4$NClO$_4$, used in the electrochemical studies was obtained from Fluka Chemicals. The syntheses of ZnCPs [9d] and compound **2**[5g] are given elsewhere.

Instrumentation: The UV/Vis spectral measurements were carried out by using a Shimadzu Model 1600 UV/Vis spectrophotometer. NIR measurements were performed by using a Cary NIR or a JASCO UV/Vis-NIR spectrophotometer. The steady-state fluorescence emission was monitored by using a Varian Cary Eclipse spectrometer. A right-angle detection method was used. The ^{1}H NMR studies were carried out by using a Varian 400 MHz spectrometer. Tetramethylsilane (TMS) was used as an internal standard. Cyclic voltammograms were recorded by using an EG&G PARSTAT electrochemical analyzer with a three electrode system in solvents that contained 0.1 M nBu$_4$NClO$_4$ as the supporting electrolyte. A platinum button or glassy carbon electrode was used as the working electrode. A platinum wire served as the counter electrode and Ag/AgCl was used as the reference electrode. All of the solutions were purged prior to spectral measurements being recorded by using argon gas. The electrospray ionization (ESI) mass spectral analyses were performed by using a Fennigan LCQ-Deca mass spectrometer.

TEM samples of the carbon nanotubes were obtained by adding isopropanol and sonicating the suspension for 5 min. Samples were placed onto a carbon-coated copper grid. TEM and energy-dispersive X-ray spectroscopy (EDX) experiments were performed by using a JEOL electron microscope (JEM-2010F FasTEMm FEI) operating at 200 kV with an extracting voltage of 4500 V at the Research Resources Center, UIC, Chicago. The copper grid (200 mesh, Cu PK/100) was supplied by SPI supplies, USA.

Time-resolved emission and transient absorption measurements: The picosecond time-resolved fluorescence spectra were measured by using an argon ion pumped Ti/sapphire laser (Tsunami; pulse width = 2 ps) and a streak scope (Hamamatsu Photonics; response time = 10 ps). The details of the experimental setup are described elsewhere.[16] Nanosecond transient absorption measurements were carried out by using an Nd/YAG laser (Spectra Physics, Quanta-Ray GCR-130, fwhm 6 ns) as the excitation source. For the transient absorption spectra in the NIR region (600–1600 nm), the monitoring light from a pulsed Xe lamp was detected with a Ge-avalanche photodiode (Hamamatsu Photonics, B2834).[16]

Synthesis of alkyl ammonium functionalized pyrene 1

N-*Boc-(2-amino)ethylamine (**3**, Boc:* t-*butyloxycarbonyl)*: This compound was prepared according to Muller et al.[17] Di-*tert*-butyl bicarbonate (6.53 g, 0.03 mol) dissolved in dry $CHCl_3$ (100 mL) was added to a solution of ethylenediamine (20 mL, 0.3 mol) in $CHCl_3$ (300 mL) over 2.5 h with stirring and cooling in an ice bath. The reaction mixture was stirred for an additional 24 h at room temperature and was then washed with water, extracted with $CHCl_3$, and dried over anhydrous Na_2SO_4. Evaporation of the organic layer yielded the desired compound as a pale yellow oil (5.2 g, 11%). ^{1}H NMR ($CDCl_3$): $\delta = 5.28$ (br s, 1H; −NH), 3.25–3.08 (m, 2H; CH_2), 2.80 (t, 2H; CH_2), 1.65–1.40 ppm (m, 9H; Boc-*H*).

N-*[2-(*N*-Boc)aminoethyl]-4-pyreneyl butanamide (**4**)*: 1-Pyrene butyric acid (400 mg, 1.4 mmol) and **3** (290 mg, 1.8 mmol) were dissolved in dry CH_2Cl_2 (50 mL) before 1,3-dicyclohexycarbodiimide (373.46 mg, 1.8 mmol) and 4-(dimethylamino) pyridine (56.2 mg, 0.46 mmol) were added and the reaction mixture was stirred for 24 h. Subsequently, the solvent was evaporated under reduced pressure and the crude compound was purified over a silica gel column by using $CHCl_3$/ ethyl acetate (60:40

v/*v*) as the eluent (210 mg, 35%). ^{1}H NMR (400 MHz, $CDCl_3$, 25°C, TMS): $\delta = 8.29$ (d, 1H; pyrene−*H*), 8.18–8.14 (m, 2H; pyrene−*H*), 8.13–8.08 (m, 2H; pyrene−*H*), 8.05–7.97 (m, 3H; pyrene−*H*), 7.85 (d, 1H; pyrene−*H*), 6.12 (brs, 1H; −NH), 4.88 (brs, 1H; −NH), 3.45–3.30 (m, 4H; pyrene−CH_2 *H*, ethyl−CH_2*H*), 3.30–3.22 (m, 2H; ethyl−CH_2*H*), 2.32 (t, 2H; pyrene−CH_2*H*), 2.25–2.15 (m, 2H; pyrene−CH_2*H*), 1.36 ppm (s, 9H; Boc−*H*).

Compound ***1***: Trifluoroacetic acid (5 mL) was added to a solution of **4** (100 mg, 0.23 mol) in CH_2Cl_2 (50 mL) and the mixture was stirred for 3 h at room temperature. The solvent and excess acid were removed under reduced pressure. The compound was washed three times with CH_2Cl_2 (10 mL) to remove the unreacted starting material and dried. Compound **1** was obtained as a yellowish brown solid (102 mg, 99%). ^{1}H NMR (400 MHz, $CDCl_3$, 25°C, TMS): $\delta = 8.20$ (d, 1H; pyrene−*H*), 8.08–8.05 (m, 2H; pyrene−*H*), 8.00–7.96 (m, 2H; pyrene−*H*), 7.93–7.87 (m, 3H; pyrene−*H*), 7.74 (d, 1H; pyrene−*H*), 3.44 (t, 2H; pyrene−CH_2*H*), 3.26 (t, 2H; ethyl−CH_2*H*), 3.04 (t, 2H; ethyl−CH_2*H*), 2.35 (t, 2H; pyrene−CH_2*H*), 2.15–2.05 ppm (m, 2H; pyrene−CH_2*H*).

Preparation of SWNT–1 conjugates: Purified SWNT (1.8 mg) was added to a solution of **1** (3.7 mg) dissolved in dry DMF (15 mL) and the reaction mixture was stirred for 48 h at room temperature. The resulting mixture was sonicated (Fisher Scientific, 60 Hz, 40 W) for 6 h at 20°C followed by centrifugation (Fisher Scientific, 50/60 CY) for 2 h. Excess **1** was removed by separating the yellow colored centrifugate from the black precipitate. Further purification was carried out by dissolving the black mixture in fresh DMF (5 mL), sonicating for 30 min at 20°C, followed by centrifugation for 1 h. Then, unadsorbed **1** was separated from the black centrifugate. This process was repeated (at least twice) until the solution in the centrifuge tube turned colorless. Finally, fresh solvent (10 mL) was added to the resulting deposit and then the suspension was sonicated for 15 min at 20°C. This homogenous black dispersion was stable at room temperature and used for the above mentioned studies.

Acknowledgement

This work is supported by the National Science Foundation (Grant 0453464 to F.D.).

[1] a) *Carbon Nanotubes: Synthesis, Structure, Properties and Applications* (Eds.: M. S. Dresselhaus, G. Dresselhaus, P. Avouris), Springer, Berlin, **2001**; b) S. Reich, C. Thomsen, J. Maultzsch, *Carbon Nanotubes: Basic Concepts and Physical Properties*, Wiley-VCH, Weinheim, **2004**; c) P. Harris, *Carbon Nanotubes and Related Structures: New Materials for the Twenty-First Century*, Cambridge University Press, Cambridge, **2001**.

[2] a) For a special issue on carbon nanotubes, see *Acc. Chem. Res.* **2002**, *35*, 997; b) D. M. Guldi, G. M. A. Rahman, E. Vito, C. Ehli, *Chem. Soc. Rev.* **2006**, *35*, 471; c) *Introduction to Nanotechnology*, (Eds.: C. P. Poole, F. J. Owens), Wiley-VCH, Weinheim, **2003**; d) *Nanophysics and Nanotechnology: An Introduction to Modern Concepts in Nanoscience* (Ed.: E. L. Wolf), Wiley, New York, **2004**; e) *Nanoarchitectures and Nanostructured Materials*, (Eds.: Y. Champion, H.-J. Fecht), Wiley-VCH, Weinheim, **2004**.

[3] For selected reviews, see a) P. M. Ajayan, *Chem. Rev.* **1999**, *99*, 1787; b) A. Hirsch, *Angew. Chem.* **2002**, *114*, 1933; *Angew. Chem. Int. Ed.* **2002**, *41*, 1853; c) Y.-P. Sun, K. Fu, Y. Lin, W. Huang, *Acc. Chem. Res.* **2002**, *35*, 1096.

[4] For selected examples, see a) V. Georgakilas, K. Kordatos, M. Prato, D. M. Guldi, M. Holzinger, A. Hirsch, *J. Am. Chem. Soc.* **2002**, *124*, 760; b) H. Murakami, T. Nomura, N. Nakashima, *Chem. Phys. Lett.* **2003**, *378*, 481; c) H. Li, B. Zhou, L. Gu, W. Wang, K. A. Shiral Ferando, S. Kumar, L. F. Allard, Y.-P. Sun, *J. Am. Chem. Soc.* **2004**, *126*, 1014; d) D. M. Guldi, M. Marcaccio, D. Paolucci, F. Paolucci, N. Tagmatarchis, D. Tasis, E. Vozquez, M. Prato, *Angew. Chem.* **2003**, *115*, 4243; *Angew. Chem. Int. Ed.* **2003**, *42*, 4206; e) R. J. Chen, Y. Zhang, D. Wang, H. Dai, *J. Am. Chem. Soc.* **2001**, *123*, 3838; f) D. Pantarotto, C. D. Partidos, R. Graff, J. Hoebeke, J.-P. Briand, M. Prato, A. Bianco, *J. Am. Chem. Soc.* **2003**, *125*, 6160; g) M. Shim, N. W. S. Kim, R. J. Chen, Y. Li, H. Dai, *Nano Lett.* **2002**, *2*, 285; h) M. A. Herranz, N. Martin, S. Campidelli, M. Prato, G. Brehm, D. M. Guldi, *Angew. Chem.* **2006**, *118*, 4590; *Angew. Chem. Int. Ed.* **2006**, *45*, 4478; i) K. Saito, V. Troiani, H. Quin, N. Solladie, T. Sakata, H. More, M. Ohama, S. Fukuzumi, *J. Phys. Chem. C* **2007**, *111*, 1194; j) D. S. Hecht, R. A. J. Ramieerz, M. Briman, E. Artukovic, K. S. Chichak, J. F. Stoddart, G. Gruner, *Nano Lett.* **2006**, *6*, 2031; k) P. J. Boul, D.-G. Cho, G. M. A. Rahman, M. Marquez, Z. Ou, K. M. Kadish, D. M. Guldi, J. L. Sessler, *J. Am. Chem. Soc.* **2007**, *129*, 5683.

[5] a) D. M. Guldi, G. M. A. Rahman, N. Jux, N. Tagmatarchis, M. Prato, *Angew. Chem.* **2004**, *116*, 5642; *Angew. Chem. Int. Ed.* **2004**, *43*, 5526; b) D. M. Guldi, G. M. A. Rahman, M. Prato, N. Jux, Sh. Qin, W. Ford, *Angew. Chem.* **2005**, *117*, 2051; *Angew. Chem. Int. Ed.* **2005**, *44*, 2015; c) D. M. Guldi, H. Taieb, G. M. A. Rahman, N. Tagmatarchis, M. Prato, *Adv. Mater.* **2005**, *17*, 871; d) D. M. Guldi, G. M. A. Rahman, N. Jux, D. Balbinot, U. Hartnagel, N. Tagmatarchis, M. Prato, *J. Am. Chem. Soc.* **2005**, *127*, 9830; e) D. M. Guldi, G. M. A. Rahman, S. Qin, M. Tchoul, W. T. Ford, M. Marcaccio, D. Paolucci, F. Paolucci, S. Campidelli, M. Prato. *Chem. Eur. J.* **2006**, *12*, 2152; f) M. Alvari, P. Atienzar, P. De la Cruz, J. L. Juan, V. Troiani, H. Garcia, F. Langa, A. Palkar, L. Echegoyen, *J. Am. Chem. Soc.* **2006**, *128*, 6626; g) T. Hasobe, S. Fukuzumi, P. V. Kamat, *J. Phys. Chem. B* **2006**, *110*, 25477; h) R. Chitta, A. S. D. Sandanayaka, A. L. Schumacher, L. D'Souza, Y. Araki, O. Ito, F. D'Souza, *J. Phys. Chem. C* **2007**, *111*, 6947.

[6] For special issues on H-bonded self-assembled systems, see a) A. J. Barnes, H. Ratajczak, *J. Mol. Struct.* **1997**, *413*, issues 1–3; b) I. Bouamaied, T. Coskun, E. Stulz, *Structure and Bonding*, **2006**, *121*, 1–147; c) L. Sánchez, N. Martín, D. M. Guldi, *Angew. Chem.* **2005**, *117*, 5508; *Angew. Chem. Int. Ed.* **2005**, *44*, 5374; d) J. Rebek, Jr. *Chem. Soc. Rev.* **1996**, *25*, 255; e) F. Diederich, M. Gomez-Lopez, *Chem. Soc. Rev.* **1999**, *28*, 263; f) M. J. Gunter, *Eur. J. Org. Chem.* **2004**, 1655.

[7] R. J. Chen, Y. Zhang, D. Wang, H. Dai, *J. Am. Chem. Soc.* **2001**, *123*, 3838.

[8] H. A. Benesi, J. H. Hildebrand, *J. Am. Chem. Soc.* **1949**, *71*, 2703.

[9] a) N. Solladié, M. E. Walther, M. Gross, T. M. F. Duarte, C. Bourgogne, J.-F. Nierengarten, *Chem. Commun.* **2003**, 2412; b) F. D'Souza, R. Chitta, S. Gadde, M. E. Zandler, A. S. D. Sandanayaka, Y. Araki, O. Ito, *Chem. Commun.* **2005**, 1279; c) F. D'Souza, R. Chitta, S. Gadde, M. E. Zandler, A. S. D. Sandanayaka, Y. Araki, O. Ito, *Chem. Eur. J.* **2005**, *11*, 4416; d) U. Hahn, M. Elhabiri, A. Trabolsi, H. Herschbach, E. Leize, A. Van Dorsselaer, A. M. Albrecht-Gray, J. F. Nierengarten, *Angew. Chem.* **2005**, *117*, 5472; *Angew. Chem. Int. Ed.* **2005**, *44*, 5338; e) F. D'Souza, R. Chitta, S. Gadde, A. L. McCarty, P. A. Karr, M. E. Zandler, A. S. D. Sandanayaka, Y. Araki, O. Ito, *J. Phys. Chem. B* **2006**, *110*, 5905; f) J.-F. Nierengarten, U. Hahn, T. M. F. Duarte, F. Cardinali, N. Solladie, M. E. Walther, A. Van Dorsselaer, H. Herschbach, E. Leize, M.-M. Albrecht-Gary, A. Trabolsi, M. Elhabiri, *C. R. Chemie* **2006**, *9*, 1022; g) F. D'Souza, R. Chitta, S. Gadde, L. M. Rogers, P. A. Karr, M. E. Zandler, A. S. D. Sandanayaka, Y. Araki, O. Ito, *Chem. Eur. J.* **2007**, *13*, 916.

[10] M. A. Hamon, M. E. Itkis, S. Niyogi, T. Alvaraez, C. Kuper, M. Menon, R. C. Haddon, *J. Am. Chem. Soc.* **2001**, *123*, 11292.

[11] a) P. Diao, Z. Liu, B. Wu, X. Nan, J. Zhang, Z. Wei, *ChemPhysChem* **2002**, *3*, 898; b) I. Heller, J. Kong, K. A. Williams, C. Dekker, S. G. Lemay, *J. Am. Chem. Soc.* **2006**, *128*, 7353.

[12] D. Rehm, A. Weller, *Isr. J. Chem.* **1970**, 8, 259.

[13] a) S. Fukuzumi, T. Suenobu, M. Patz, T. Hirasaka, S. Itoh, M. Fujitsuka, O, Ito, *J. Am. Chem. Soc.* **1998**, *120*, 8060; b) G. Pagona, A. S. D. Sandanayaka, Y. Araki, J. Fan, N. Tagmatarchis, M. Yudasaka, S. Ijima, O. Ito, *J. Phys. Chem. B* **2006**, *110*, 20729.

[14] A. S. D. Sandanayaka, Y. Takaguchi, T. Uchida, Y. Sako, Y. Morimoto, Y. Araki, O. Ito, *Chem. Lett.* **2006**, *35*, 1188.

[15] M. A. Hamon, M. E. Itkis, S. Niyogi, T. Alvaraca, C. Kuper, M. Menon, R. C. Haddon, *J. Am. Chem. Soc.* **2001**, *123*, 11292.
[16] a) K. Matsumoto, M. Fujitsuka, T. Sato, S. Onodera, O. Ito, *J. Phys. Chem. B* **2000**, *104*, 11632; b) S. Komamine, M. Fujitsuka, O. Ito, K. Morikawa, T. Miyata, T. Ohno, *J. Phys. Chem. A* **2000**, *104*, 11497; c) M. Yamazaki, Y. Araki, M. Fujitsuka, O. Ito, *J. Phys. Chem. A* **2001**, *105*, 8615.
[17] D. Muller, I. Zeltser, G. Bitan, C. Gilon, *J. Org. Chem.* **1997**, *62*, 411.

Received: April 15, 2007
Published online: July 12, 2007

